ELSEVIER

Applied Energy 71 (2002) 59–73

APPLIED ENERGY

www.elsevier.com/locate/apenergy

Correlation models of diffuse solar-radiation applied to the city of São Paulo, Brazil

Amauri P. Oliveira[a,*], João F. Escobedo[b], Antonio J. Machado[a], Jacyra Soares[a]

[a]*Group of Micrometeorology, Department of Atmospheric Science, University of São Paulo, Rua do Matão, 1226, São Paulo, SP, Brazil 05508.900*

[b]*Laboratory of Solar Radiation, Department of Environmental Science State University of São Paulo, Botucatu, SP, Brazil*

Received 10 July 2001; received in revised form 5 September 2001; accepted 8 September 2001

Abstract

Measurements of global and diffuse solar-radiation, at the Earth's surface, carried out from May 1994 to June 1999 in São Paulo City, Brazil, were used to develop correlation models to estimate hourly, daily and monthly values of diffuse solar-radiation on horizontal surfaces. The polynomials derived by linear regression fitting were able to model satisfactorily the daily and monthly values of diffuse radiation. The comparison with models derived for other places demonstrates some differences related mainly to altitude effects.

Keywords: Diffuse solar radiation; Clearness index; Correlation modelling; São Paulo City

Introduction

A knowledge of temporal and spatial variations of global solar-radiation at the Earth's surface—and its diffuse and direct components—is crucial to climate and agricultural studies, to estimate the efficiency of solar energy collectors and several other applications [1]. There are, however, several difficulties in measuring these quantities or in estimating them with numerical modeling techniques.

With reference to the observations, the major difficulties are due to operational problems of radiation sensors and with the small number of stations in most of

* Corresponding author. Tel.: +55-11-3818-4701; fax: +55-011-3818-4714.
E-mail address: apdolive@usp.br (A.P. de Oliveira).

0306-2619/02/$ - see front matter
PII: S0306-2619(01)00040-X

Nomenclature

Abbreviations

MBE	mean bias error
RMSE	root mean square error

Symbols

A_n	polynomial coefficient
A_n^d	polynomial coefficient related to daily average
A_n^h	polynomial coefficient related to hourly average
A_n^m	polynomial coefficient related to monthly average
d_i	deviation between the ith calculated value and the ith measured value
E_{DF}	diffuse energy component at the Earth's surface, per unit of area and per time period
E_{DF}^d	diffuse energy component at the Earth's surface, per unit of area and per day
E_{DF}^h	diffuse energy component at the Earth's surface, per unit of area and per hour
E_{DF}^m	diffuse energy component at the Earth's surface, per unit of area and per month
E_G	total flux of energy received from the Sun at the Earth's surface, per unit of area and per time period
E_G^d	total flux of energy received from the Sun at the Earth's surface, per unit of area and per day
E_G^h	total flux of energy received from the Sun at the Earth's surface, per unit of area and per hour
E_G^m	total flux of energy received from the Sun at the Earth's surface, per unit of area and per month
E_T	flux of solar radiation received at the top of the atmosphere, per unit of area and per time period
E_T^d	flux of solar radiation received at the top of the atmosphere, per unit of area and per day
E_T^h	flux of solar radiation received at the top of the atmosphere, per unit of area and per hour
E_T^m	flux of solar radiation received at the top of the atmosphere, per unit of area and per month
$K_{DF} = E_{DF}/E_G$	diffuse fraction
$K_{DF}^d = E_{DF}^d/E_G^d$	daily value of diffuse fraction
$K_{DF}^h = E_{DF}^h/E_G^h$	hourly value of diffuse fraction
$K_{DF}^m = E_{DF}^m/E_G^m$	monthly value of diffuse fraction
$K_T = E_G/E_T$	clearness index
$K_T^d = E_G^d/E_T^d$	daily value of clearness index
$K_T^h = E_G^h/E_T^h$	hourly value of clearness index

$K_T^m = E_G^m / E_T^m$	monthly values of clearness index
N	polynomial order
N	total number of observations
t_c	critical value of t_s
t_S	t-statistic
Greeks	
α	level of significance

solarimetric networks worldwide. Regarding numerical modeling, the difficulty is related to the appropriate representation of cloud effects [2].

These problems are particularly severe in tropical regions, like Brazil, where cloud activity is a dominant feature of local climate and the solarimetric network is sparse with most of the stations located in urban areas [3,4]. One practical alternative is to estimate the diffuse component of solar radiation from empirical relationships derived from statistical analyses of direct and global solar radiation temporal series observed at the Earth's surface [5–9].

These models are based on the strong correlation between hourly, daily and monthly values of clearness index (K_T) and diffuse fraction (K_{DF}). They are, in general, expressed in terms of 1st to 4th-degree polynomials dependent on latitude, precipitable water content, atmospheric turbidity, surface albedo, altitude and solar elevation angle [10,11].

Most of the correlation models were derived for temperate climates [9] and tropical latitudes [8,12] located in the Northern Hemisphere. According to the literature, no correlation model has been derived for any region in South America. Oliveira et al. [4] validated a set of empirical expressions to simulate: (a) annual variations of monthly-averaged hourly values of global and diffuse solar radiation at the Earth's surface and (b) annual variation of monthly-averaged daily values of global solar radiation for São Paulo City. In case (a) the empirical expressions were straightforward interpolations of observed diurnal evolution. Case (b) used the Ängstrom formula. Despite the good performance, these models could only be applied to estimate monthly-averaged values of diffuse solar-radiation.

In this paper, global and diffuse solar radiation measurements carried out during 62 months are used to derive correlation models to estimate hourly, daily and monthly values of diffuse solar radiation in São Paulo City. The performance of these models is objectively tested using mean bias error (MBE), root mean square error (RMSE) and t-statistic (t_S) analyses [13].

Site and instrumentation

Global and diffuse solar radiations have been regularly measured in São Paulo City, Brazil, since May 1994 by a set of pyranometers and a shadow-band device, named the "movable detector device". In this device, the ring is fixed and the

annual variation of the shadow position is followed by displacing the detector horizontally. The ring is sloped northward with an angle equal to the local latitude and the detector is moved in the plane of displacement, manually, by a screw mechanism that allows one to centralize the detector under the shadow of the ring [14].

All measurements were taken on a platform located at the top of the "Instituto de Astronomia, Geofisica e Ciencias Atmosfericas da Universidade de São Paulo" building at the University Campus in São Paulo, western side, at 744 m above mean sea-level (23°33′35″ S, 46°43′55″ W) with a sampling frequency of 0.2 Hz (12 min) and stored at 5 min intervals.

The solar radiation data set used in this work comprises the period of 62 months from 1 May 1994 to 30 June 1999. All data were checked, questionable data removed, and the shadow-band blocking effects on the diffuse solar-radiation values were taken into consideration [4,14].

In this work, the total flux of energy received from the Sun, per unit of area and per hour, day or month time interval are indicated by E_G^h, E_G^d and E_G^m, respectively. The subscript G refers to global radiation and the superscripts h, d and m to hour, day and month, respectively. Equivalent symbols are used to indicate the diffuse component at the Earth's surface $\left(E_{DF}^h, E_{DF}^d, E_{DF}^m\right)$ and the flux of solar radiation received at the top of the atmosphere $\left(E_T^h, E_T^d, E_T^m\right)$. The hourly, daily and monthly values of the diffuse fraction are indicated, respectively, by K_{DF}^h, K_{DF}^d and K_{DF}^m. They are defined as E_{DF}^h/E_G^h, E_{DF}^d/E_G^d and E_{DF}^m/E_G^m, respectively. Similarly, the hourly, daily and monthly values of the clearness index are indicated by K_T^h, K_T^d and K_T^m and defined as E_G^h/E_T^h, E_G^d/E_T^d and E_G^m/E_T^m, respectively.

Correlation models for E_{DF}

The correlation between diffuse fraction and clearness index is displayed in terms of K_T–K_{DF} scatter diagrams [9]. The hourly values of K_T^h–K_{DF}^h scatter diagrams (Figs. 1 and 2) are based on 15,258 pairs of points selected from a total of 16,041 h of observation. The scatter diagrams of daily values of K_T^m–K_{DF}^m (Figs. 3 and 4) are based on 1292 pairs of points selected from 1354 days of observation. Monthly values of K_T^m–K_{DF}^m scatter diagrams (Figs. 5 and 6) are based on 60 pairs of points selected from 62 months of observation. In these diagrams, the block average was estimated taking 20 equally-spaced intervals of K_T (each interval of 0.05) and computing the average value of K_{DF} corresponding to the K_T values within these intervals. The K_{DF} block average values are indicated by open squares in Figs. 1, 3 and 5 and they correspond to the entire period of observation (62 months). The variation of K_{DF}, around each mean value, is given by twice the standard deviation error and is indicated by horizontal bars in Figs. 2, 4 and 6.

The K_T–K_{DF} diagrams displayed in Figs. 1, 3 and 5 show a good correlation between these two parameters for São Paulo City. A similar result has been found for other places for hourly, daily and monthly values [5–7,9]. The distribution of hourly and daily values of K_{DF} around the adjusted polynomial is not symmetric in the interval of $0 < K_T < 0.2$ (Figs. 1 and 3), and shows a concentration around values

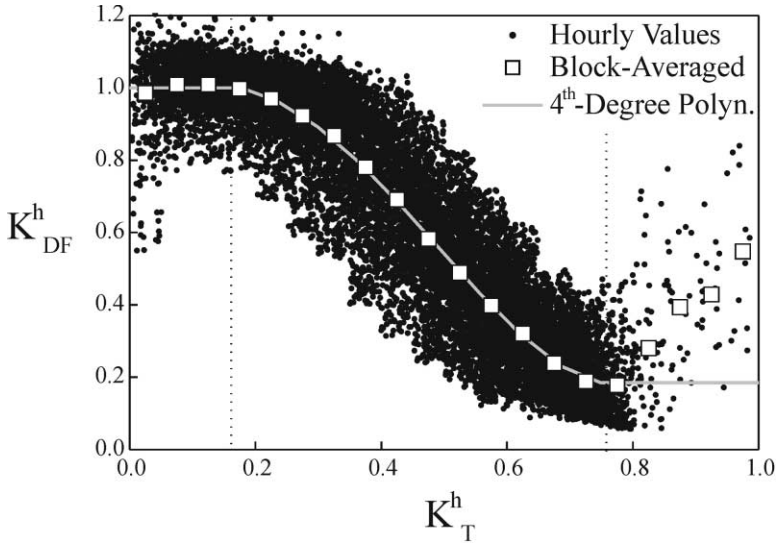

Fig. 1. K_T^h–K_{DF}^h scatter diagram for hourly values of solar radiation observed in São Paulo City during the 62 months (solid circles) and the corresponding block-averaged values (open squares). The continuous displays the 4th-degree polynomial curve. The vertical (dotted lines) indicate the interval of validity of the interpolation.

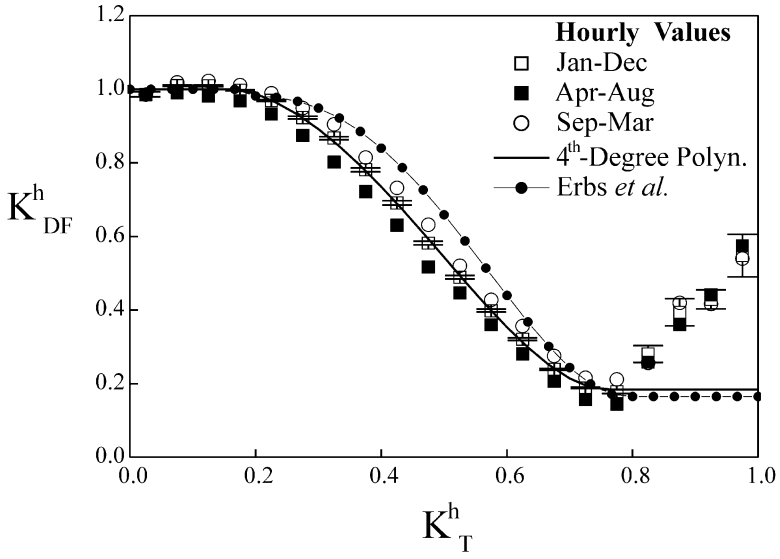

Fig. 2. K_T^h–K_{DF}^h scatter diagram for the block-averaged hourly values of solar radiation observed in São Paulo City during all 62 months (open squares), during fall–winter months (solid squares) and during spring–summer months (open circles). The 4th-degree polynomial (continuous line) was obtained using 62-month data. Erbs et al. [7] used data of four USA locations (latitudes between 31°N and 42°N) and one in Australia (38°S). The statistical errors of K_T^h are displayed as horizontal bars.

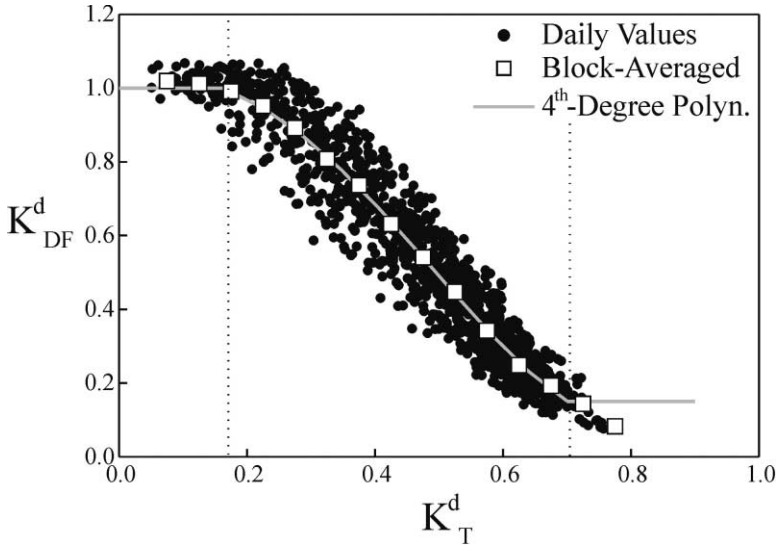

Fig. 3. K_T^d–K_{DF}^d scatter diagram for daily values of solar radiation observed in São Paulo City during all 62 months (solid circles) and the corresponding block-averaged values (open squares). The continuous line displays the 4th-degree polynomial curve. The vertical (dotted lines) indicate the interval of validity of the interpolation.

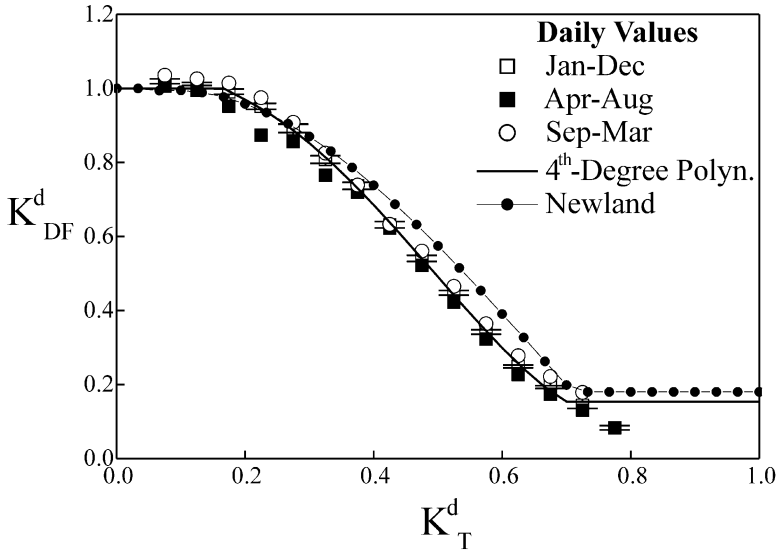

Fig. 4. K_T^d–K_{DF}^d scatter diagram for the block-averaged daily values of solar radiation observed in São Paulo City during all 62 months (open squares), during fall–winter months (solid squares) and during spring–summer months (open circles). The 4th-degree polynomial (continuous line) was obtained using 62-month data. The study of Newland [12] was performed for Macau (22.3°N). The statistical errors of K_T^d are displayed as horizontal bars.

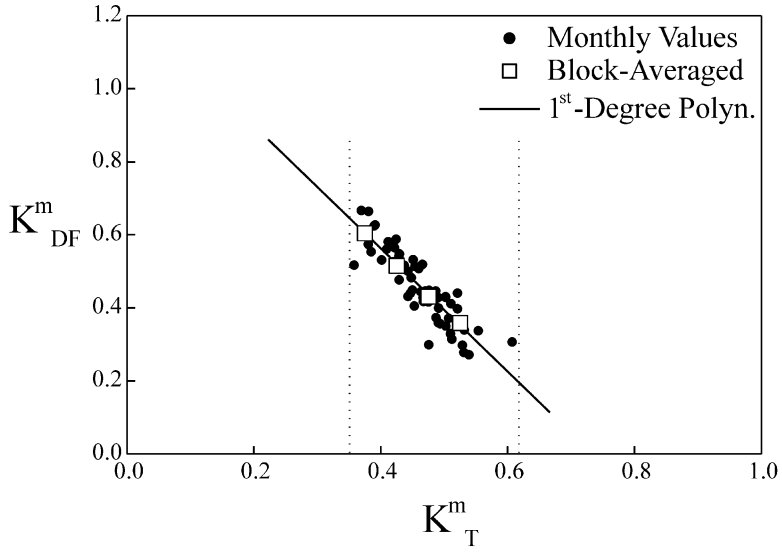

Fig. 5. K_T^m–K_{DF}^m scatter diagram for monthly values of solar radiation observed in São Paulo City during all 62 months (solid circles) and the corresponding block-averaged values (open squares). The continuous line displays the 1st-degree polynomial curve. The vertical (dotted lines) indicate the interval of validity of the interpolation.

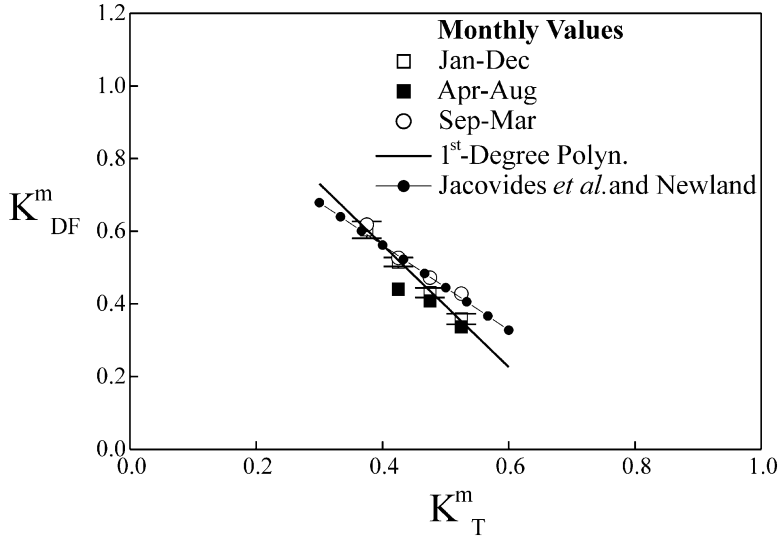

Fig. 6. K_T^m–K_{DF}^m scatter diagram for the block-averaged monthly values of solar radiation observed in São Paulo City during all 62 months (open squares) during fall–winter months (solid squares) and during spring–summer months (open circles). The 1st-degree polynomial curve (continuous line) was obtained using 62-month data. The studies of Newland [12] and Jacovides et al. [9] were performed, respectively, for Macau (22.3°N) and the island of Cyprus (25°N). The statistical errors of K_{DF}^m are displayed as horizontal bars.

slightly higher than unity. This tendency, less pronounced for hourly values (Fig. 1), could be produced by the correction of shadow-band blocking on the diffuse solar radiation measurements during totally cloudy days [4]. In Figs. 1 and 2, K_{DF}^{h} exhibits a secondary maximum for $K_T^h \to 1.0$. This is a common feature for hourly value correlation curves and has been observed in other places [12,15]. It is related to a systematic increase in diffuse solar radiation caused by surface and cloud reflections at the end of the day, when the Sun is not totally obscured by the horizon [12].

The solar radiation mean behavior during fall–winter months (considered here to be April to August) and spring–summer months (considered here to be September to March) are indicated in Figs. 2, 4 and 6. According to Oliveira et al. [4], during the fall–winter months, the climate in São Paulo City is drier and colder than in spring–summer months. For a given value of K_T, the corresponding K_{DF} in the spring–summer period is higher than the corresponding K_{DF} considering all months of the year. On the other hand, for a given value of K_T, the corresponding K_{DF} in the fall–winter period is lower than the corresponding K_{DF} considering all months of the year. This contrast is statistically significant for hourly and daily values of K_{DF}, according to the error bars in Figs. 2 and 4.

This pattern indicates that the diffuse fraction in São Paulo during warmer and wetter months is larger than during cooler and drier ones. The explanation for this behaviour is that, during the wetter period, the cloud activity is more intense and the atmospheric water content is larger than during the drier period so yielding comparatively larger values of E_{DF}^{h}, E_{DF}^{d}, E_{DF}^{m} for the same values of E_T^h, E_T^d, E_T^m. This effect has also been observed in several other place [6,7,12].

To obtain an expression to estimate hourly, daily and monthly values of diffuse solar radiation from observed global solar radiation, a set of polynomials is fitted through the data points in all three K_T–K_{DF} diagrams (Figs. 2, 4 and 6). The generic n^{th}-degree polynomial will have the following characteristic:

$$K_{DF} = \sum_{n=0}^{N} A_n (K_T)^n \tag{1}$$

where A and n are, respectively, the coefficient and the order of the polynomial.

In this work, a 4$^{\text{th}}$-degree polynomial was used for hourly and daily values, while for monthly values a 1st-degree polynomial was utilized. This choice is based on the fact that most of the expressions, available in the literature, are 4$^{\text{th}}$ and 1$^{\text{st}}$-degree polynomials [7,9,12]. So, the use of these polynomial degrees allows a straight-forward comparison with previous works. The coefficients of expression (1) applied to the 62 months of observations and their respective intervals of validity are given in Table 1.

In Figs. 1–6, the continuous lines correspond to the fitted curves throughout the pairs of points (K_T, K_{DF}) considering observations carried out in São Paulo during all 62 months of observation. The vertical dotted lines in Figs. 1, 3 and 5 define the interval of validity for each polynomial curve.

The hourly and daily values of the validity intervals were chosen considering the interception of 4th-degree polynomial curves with the two asymptotic limits of K_{DF}. When $K_T \to 0$ (cloudy condition), it is assumed that $K_{DF} \to 1$; on the other hand,

Table 1
Coefficients of the polynomial curves obtained from linear regressions in the K_T–K_{DF} diagrams for hourly, daily and monthly values of solar radiation observed in São Paulo City

Period of observation	Hourly values (K_T^h–K_{DF}^h diagram in Fig. 2)						
	A_0^h	A_1^h	A_2^h	A_3^h	A_4^h	Interval of validity	$(K_{DF}^h)_{\min}$
January–December	0.97	0.80	−3.0	−3.1	5.2	$0.17 < K_T^h < 0.75$	0.18
April–August	0.97	0.48	−2.7	−2.7	4.7	$0.17 < K_T^h < 0.75$	0.17
September–March	0.96	0.92	−3.0	−3.4	5.2	$0.25 < K_T^h < 0.75$	0.21
Literature							
Erbs et al. [7]	0.95	−0.16	4.4	−16.	12.	$0.22 < K_T^h < 0.80$	0.17
	Daily values (K_T^d–K_{DF}^d diagram in Fig. 4)						
	A_0^d	A_1^d	A_2^d	A_3^d	A_4^d	Interval of validity	$(K_{DF}^d)_{\min}$
January–December	1.0	0.27	−2.5	−2.6	4.3	$0.17 < K_T^{1d} < 0.70$	0.15
April–August	1.0	0.07	−1.9	−2.9	4.1	$0.10 < K_T^{1d} < 0.70$	0.13
September–March	1.1	0.23	−2.6	−2.2	4.3	$0.20 < K_T^{1d} < 0.70$	0.19
Literature							
Newland [12]	0.97	0.56	−3.4	1.0	0.51	$0.10 < K_T^{1d} < 0.71$	0.18
	Monthly values (K_T^m–K_{DF}^m diagram in Fig. 6)						
	A_0^m	A_1^m	A_2^m	A_3^m	A_4^m	Interval of validity	$(K_{DF}^m)_{\min}$
January–December	1.2	−1.7	–	–	–	$0.35 \leqslant K_T^m \leqslant 0.61$	0.30
April–August	0.88	−1.0	–	–	–	$0.44 \leqslant K_T^m \leqslant 0.61$	0.34
September–March	1.1	–1.3	–	–	–	$0.35 \leqslant K_T^m \leqslant 0.61$	0.30
Literature							
Newland [12]	1.0	−1.2	–	–	–		
Jacovides et al. [9]	1.0	−1.2	–	–	–		

when $K_T \to 1$ (clear-sky condition), it is assumed that $K_{DF} \to (K_{DF})_{\min}$. The minimum value of K_{DF} was set equal to the minimum block-averaged value (Figs. 1 and 3). For monthly values (Fig. 5), the validity interval was given by the range of the data set used in the fitting process. These procedures were also performed for the polynomials adjusted to fall–winter and spring–summer months (Table 1).

The polynomial curves for São Paulo are compared with other locations in Figs. 2, 4 and 6 and the coefficients of expression (1) obtained by other authors can be compared with those derived for São Paulo in Table 1.

Considering the polynomial obtained from the correlation for hourly values using all the months of the year (Fig. 2), the São Paulo curve yields lower values of K_{DF}^h, for all values of K_T^h in the interval of validity, when compared with the averaged curve obtained by Erbs et al. [7] using data of four USA locations (latitudes between 31°N and 42.5°N) and one in Australia (38°S). The maximum difference in K_{DF}^h is 0.12 and occurs when K_T^h is equal to 0.50 (Fig. 2).

Similarly, for daily values, the annual curve for São Paulo yields lower values of K_{DF}^{d} when compared with the curve obtained by Newland [12] for Macau (22.3°N). The maximum difference, in this case, is 0.09 and occurs for K_{T}^{d} equal to 0.60 (Fig. 4)

For monthly values, the slope of the fitted curve for São Paulo (1st-degree polynomial) is larger than those obtained for Macau (22.3°N) and the Island of Cyprus (25°N) by Newland [12] and Jacovides et al. [9], respectively (Fig. 6).

Observations obtained by LeBaron and Dirmhirn [10], for high elevation terrains—1250 and 3300 m—located in middle latitude regions (Colorado, USA) yielded a steeper correlation curve for daily values, which was explained by the authors in terms of an altitude effect. This is also a plausible explanation for the discrepancies between São Paulo and other places.

According to LeBaron and Dirmhirn [10], the larger inclination is a direct consequence of: (a) the decrease in the asymptotic value of K_{DF}^{d} as the clearness index approaches unity (clear-sky condition) and (b) the increase of the lower value of K_{T}^{d} when K_{DF}^{d} is still large (cloudy condition). The cause (a) can be explained in terms of path-length reduction of the solar rays in the atmosphere while cause (b) can be attributed to an anomalous increase of the solar-radiation diffuse component at the Earth's surface due to the large frequency of towering cumulus clouds. These conditions are amplified during winter as a consequence of the albedo increase (i.e. multiple reflection associated to the presence of snow).

Indeed, modeling results obtained by Gueymard [16] for a cloudless atmosphere show that a higher atmospheric turbidity displaces the K_T–K_{DF} correlation curve upwards, i.e. for a given value of K_T an increase of turbidity increases K_{DF}^{d}. This indicates that an increase of moisture or aerosol load in the atmosphere would increase the intensity of diffuse solar-radiation at the expense of the direct component of solar radiation at the Earth's surface.

Since São Paulo is located at approximately 750 m above mean sea-level and 23.56°S, the reduction in the path length, due to altitude effects, can explain the steeper correlation curves for daily and monthly values found in this work (Figs. 4 and 6). It should be mentioned that São Paulo is characterized by frequent episodes of high levels of air pollution during the winter period (June–July).

Oliveira et al. [4] have shown that episodes of high levels of particulate-matter concentration during clear-sky days are related to an increase of diffuse solar-radiation in São Paulo. If the effect of the presence of an aerosol alone is considered, a less steep inclination in the correlation curve would be expected, whereas increasing turbidity increases K_{DF} as $K_T \to 1$. However, this interpretation is not conclusive because clear days are not necessarily polluted days. Besides, high episodes of air pollution can increase turbidity in cloudy days, so that K_{DF} can also increase when $K_T \to 0$, so attenuating the slope of the correlation curve.

Finally, the altitude effect on the correlation diagram for São Paulo City is less pronounced than the results found by LeBaron and Dirmhirn [10]. Apparently, the reason is that the albedo of the urban and non-urban areas varies less during the year in São Paulo (there is never snow in São Paulo) than in the high-elevation locales investigated by them.

For monthly values, the differences between São Paulo (23.5° S) and Macau (22.3°N) are largest during April–August (Fig. 6). Soler [11] compared the latitudinal variations of the polynomial coefficients of the expression (1), for radiation monthly values, obtained in several different places. It can be verified using expression (1) that a larger polynomial coefficient of zero order ($A_0^m = 1.2$) and a smaller polynomial coefficient of first order ($A_1^m = -1.7$) is obtained for São Paulo and becomes consistent with the expected behaviour at low latitudes achieved from a simple extrapolation of the results obtained by Soler [11] between 36°N and 61°N.

Model performance

To evaluate the performance of the diffuse solar-radiation models at the Earth's surface for São Paulo city (Table 1), a statistical comparison is performed using the indicator, proposed by Stone [13], a *t*-statistic (t_S). This indicator is used along with two other well-known parameters: MBE and RMSE. Both MBE and RMSE have been specially employed as adjustments of solar-radiation models [11,17,18]. The RMSE and the MBE are defined as follows:

$$\mathrm{MBE} = \left(\sum_{i=1}^{N} d_i / N \right) \tag{2}$$

$$\mathrm{RMSE} = \left(\sqrt[2]{\sum_{i=1}^{N} (d_i)^2 / N} \right) \tag{3}$$

Here N is the total number of observations and d_i is the deviation between the i^{th} calculated and the i^{th} measured values. The test of MBE provides information on the long-term performance of models studied. A positive MBE value gives the average amount of over-estimation in the calculated values and vice versa. In general, a small MBE is desirable. It should be noted, however, that over-estimation of an individual observation will cancel under-estimation in a separate observation. On the other hand, the test on RMSE provides information on the short-term performance of the models as it allows a term-by-term comparison of the actual deviation between the calculated value and the measured value [17]. Thus, each test by itself may not be an adequate indicator of a model's performance because it is possible to have a large value for the RMSE and, at the same time, a small value for the MBE, and vice-versa.

Therefore, Stone [13] introduced the *t*-statistic as a new indicator of adjustment between calculated and measured data. This statistical indicator allows models to be compared and, at same time, can indicate whether or not a model's estimates are statistically significant at a particular confidence level. Moreover, it can be computed using both the RMSE and MBE and takes into account the dispersion of the results, which is neglected when the RMSE and MBE are considered separately. The *t*-statistic is defined as:

$$t_S = \left(\sqrt[2]{(N-1)\mathrm{MBE}^2 / \left(\mathrm{RMSE}^2 - \mathrm{MBE}^2\right)} \right) \tag{4}$$

To determine whether a model's estimates are statistically significant one has simply to determine a critical t_c value obtainable from standard statistical tables, e.g. t_c ($\alpha/2$) at the α level of significance, and ($N-1$) degrees of freedom. For the model's estimate to be judged statistically significant at the ($1-\alpha$) confidence level, the calculated t_s value must be between the interval defined by $-t_c$ and t_c (i.e. the acceptance region under the reduced normal-distribution curve). Values outside this interval, the so-called critical region, are those for which we reject the hypothesis that the parameter selection has improved the model.

A summary of the statistical parameters is shown in Table 2 for hourly, daily and monthly values of E_{DF}. The critical values of t_s (t_c) are relative to a level of confidence of 95%.

In the case of the hourly values, all expressions derived for São Paulo performed poorly. A negative MBE indicates that the model underestimates E^h_{DF} systematically. According to Erbs et al. [7], the models obtained from hourly value correlations do not produce good results because the hourly values of global solar-radiation are very sensitive to the cloud type, which is not included in the correlation model developed here. The relatively best result was obtained when the hourly values of diffuse solar-radiation were calculated with a 4$^{\text{th}}$-degree polynomial based on the spring–summer

Table 2
Comparison between measured and modelled hourly, daily and monthly values of diffuse solar-radiation at the Earth's surface in São Paulo City

Period of observation	Hourly values (K^h_T–K^h_{DF} diagram in Fig. 1)				
	Sample size (h)	MBE (MJ/m^2)	RMSE (MJ/m^2)	t_s	t_c
January–December	15,258	−0.0169	0.193	11.16	1.96
April–August	6408	−0.0100	0.141	5.79	1.96
September–March	9633	−0.0087	0.209	4.11	1.96
	Daily values (K^d_T–K^d_{DF} diagram in Fig. 3)				
	Sample size (day)	MBE (MJ/m^2)	RMSE (MJ/m^2)	t_s	t_c
January–December	1292	−0.035	1.34	0.95	1.96
April–August	599	−0.009	0.79	0.29	1.96
September–March	755	0.048	1.58	0.84	1.96
	Monthly values (K^m_T–K^m_{DF}diagram in Fig. 5).				
	Sample size (month)	MBE (MJ/m^2)	RMSE (MJ/m^2)	t_s	t_c
January–December	60	−2.205	15.90	1.076	1.671
April–August	28	−0.088	10.82	0.043	1.701
September–March	32	−0.820	14.34	0.324	1.696

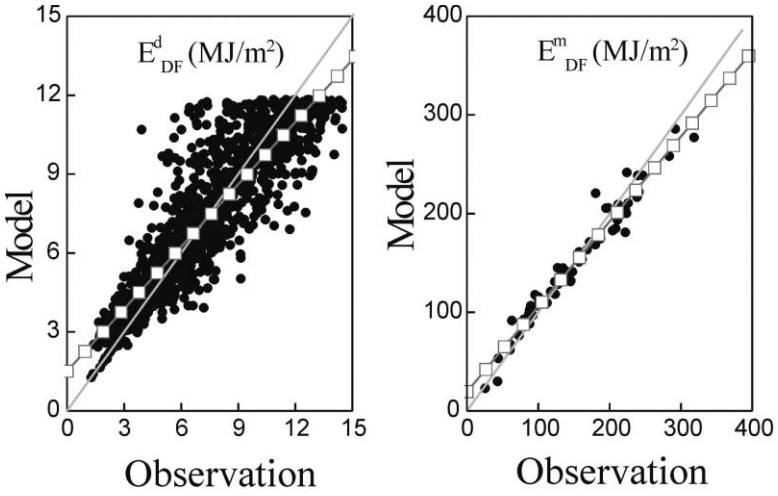

Fig. 7. scatter diagram for daily (left) and monthly (right) values of the observed versus modelled diffuse radiation in São Paulo City. The modelled values were obtained from polynomials interpolated from the observations during January–December (Table 1). The linear regression lines (open-squares) correspond to the correlation coefficients 0.90 and 0.98, respectively, for daily and monthly values of diffuse solar-radiation. The continuous lines correspond to the diagram diagonal.

months. Curiously, in this period, the cloud activity is enhanced in the City of São Paulo.

Related to the daily values (Table 2), all three 4th-degree polynomials (Table 1) are qualified to simulate the diffuse radiation at the City of São Paulo. However, they generally under-estimate the observations. The best performance is obtained in the fall–winter period (April–August). The discrepancies depend on the intensity of diffuse solar-radiation (Fig. 7, left). For instance, the polynomial derived from the whole data set (January–December, Table 1) over-estimates E^d_{DF} below 5 MJ/m^2 and underestimates E^d_{DF} above 5 MJ/m^2.

Similarly to the daily values, the performance of the 1st-degree polynomial in computing the monthly values of diffuse radiation at the Earth's surface in São Paulo is very good (Table 2). The best performance is observed for the polynomial derived for the fall–winter period (April–August). The model over-estimates E^m_{DF} below 200 MJ/m^2 and under-estimates E^m_{DF} above 200 MJ/m^2 (Fig. 7, right).

Conclusions

Measurements of global and diffuse solar-radiations at the Earth's surface in São Paulo City, between May 1994 and June 1999 are used to derive models to estimate the diffuse solar-radiation from values of global solar-radiation. These models are based on the correlation between the diffuse fraction and clearness index for hourly, daily and monthly values.

The major conclusions are:

1. the K_T–K_{DF} diagrams indicate that the diffuse fraction is strongly correlated to the clearness index for hourly, daily and monthly values of solar radiation in the City of São Paulo;
2. the overall characteristics of the diffuse-fraction correlation curves and their seasonal variations are similar to other places with equivalent latitude for hourly, daily and monthly values [7,9,12];
3. the hourly and daily K_T–K_{DF} diagrams indicated smaller values of K_{DF} for São Paulo when compared with other places, for values of K_T within 0.3 and 0.7;
4. the K_T–K_{DF} diagram for monthly values indicates a larger slope at São Paulo than elsewhere. It is assumed that these discrepancies are due to the reduction of turbidity caused by the altitude effect and higher frequency of towering cumulus clouds in the spring–summer seasons [16]. Even though the City of São Paulo is only 750 m above mean sea-level, the altitude impact on the radiative properties of its atmosphere may be significant. Another important factor which can modify the turbidity in São Paulo, is the presence of pollution. According to Oliveira et al. [4], an increase in the particulate matter concentration is followed by a decrease in global solar-radiation, but it does not affect its diffuse component at the Earth's surface. This indicates that the aerosol load in São Paulo cannot be the only reason for the observed discrepancy in the correlation curve. It is assumed that the reduction of the moisture content due to the altitude effect may be contributing in this case; and
5. the daily and monthly values of diffuse solar radiation at the Earth's surface (horizontal plane) can be estimated for São Paulo City, during all months of the year, by the following expressions:

$$K_{DF}^{d} = 1.0 + 0.27\left(K_T^d\right) - 2.5\left(K_T^d\right)^2 - 2.6\left(K_T^d\right)^3 + 4.3\left(K_T^d\right)^4$$

$$K_{DF}^{m} = 1.2 - 1.7\left(K_T^m\right)$$

The performance of the model will improve if the seasonal variations are taken into consideration in the models' data set basis.

Acknowledgements

The authors acknowledge the financial support provided by "CNPq—Conselho Nacional de Desenvolvimento Científico e Tecnológico" and by "Fapesp—Fundação de Amparo á Pesquisa do Estado de São Paulo".

References

[1] Duffie JH, Beckman WH. Solar engineering of thermal processes. , New York: Wiley Interscience, 1980.

[2] Iqbal M. An introduction to solar radiation. Academic Press, New York, 1983.
[3] Pereira EB, Abreu SL, Stuhlmann R, Reiland M, Colle S. Survey of the incident solar-radiation in Brazil by use of Meteosat satellite data. Solar Energy 1996;2:125–32.
[4] Oliveira AP, Machado AJ, Escobedo JF, Soares J. Diurnal evolution of the solar radiation in the City of São Paulo, Brazil: seasonal variation and modelling. Theoretical and Applied Climatology 2001 (in press).
[5] Liu BYH, Jordan RC. The interrelationship and characteristic distribution of direct, diffuse and total solar-radiation. Solar Energy 1960;4:1–9.
[6] Collares-Pereira M, Rabl A. The average distribution of solar radiation—correlation between diffuse and hemispherical and between daily and hourly insolation values. Solar Energy 1979;22:155–64.
[7] Erbs DG, Klein SA, Duffie JA. Estimation of the diffuse-radiation fraction for hourly, daily and monthly-average global radiation. Solar Energy 1982;28:293–302.
[8] Satyamurti VV, Lahiri PK. Estimation of symmetric and asymmetric hourly global and diffuse radiation from daily values. Solar Energy 1992;48:7–14.
[9] Jacovides CP, Hadjioannou L, Passhiardis S, Stefanou L. On the diffuse fraction of daily and monthly global-radiation for the Island of Cyprus. Solar Energy 1996;56:565–72.
[10] LeBaron B, Dirmhirn I. Strengths and limitations of the Liu and Jordan model to determine diffuse from global irradiance. Solar Energy 1983;31:167–72.
[11] Soler A. Dependence on latitude of the relation between the diffuse fraction of solar radiation and the ratio of global-to-extraterrestrial radiations for monthly average daily values. Solar Energy 1990; 44:297–302.
[12] Newland FJ. A study of solar radiation modes for the coastal region of South China. Solar Energy 1989;43:227–35.
[13] Stone RJ. Improved statistical procedure for the evaluation of solar-radiation estimation models. Solar Energy 1993;51:289–91.
[14] Oliveira AP, Escobedo JF, Machado AJ. A new shadow-ring device for measuring diffuse solar-radiation at the surface. Journal of Atmospheric and Oceanic Technology 2001 (in press).
[15] Skartveit A, Olseth JA. A model for the diffuse fraction of hourly global radiation. Solar Energy 1987;38:271–4.
[16] Gueymard C. A two-band model for the calculation of clear-sky solar irradiance, illuminance, and photosynthetically active radiation at the Earth's surface. Solar Energy 1989;44:253–65.
[17] Halouani N, Ngguyen CT, Vo-Ngoc D. Calculation of monthly average global solar radiation on horizontal surfaces using daily hours of bright sunshine. Solar Energy 1993;50(3):247–58.
[18] Ma CCY, Iqbal M. Statistical comparison of solar-radiation correlations. Monthly average global and diffuse radiation on horizontal surfaces. Solar Energy 1984;33(2):143–8.